International Journal of Advances in Engineering and Management (IJAEM)
Volume 4, Issue 4Apr 2022, pp: 357-371www.ijaem.net ISSN: 2395-5252

Two-Dimensional Dissipative Non-Slip MHD Flow of Arrhenius Chemical Reaction with Variable Properties

Akindele M. Okedoye*, Kelvin O. Ogboru, John Damisa and, Beauty. B. Malemi

Department of Mathematics, Federal University of Petroleum Resources, Effurun, NIGERIA.

Submitted: 01-04-2022 Revised: 06-04-2022 Accepted: 11-04-2022

ABSTRACT: The aim of this paper is to study two-dimensional dissipative non-slip MHD flow of Arrhenius chemical reaction with variable properties**.** The governing equations are simplified to non-dimensional form and linearized in order Reynold number. The resulting coupled equations are solved numerically using Maple inbuilt solver, the characteristics of the flow are obtained as well as the effect of the flow governing parameters were examined graphically and discussed to pinpoint their influence on the flow. It was discovered that even at low Reynold number, transfer of non-linear energy and specie concentration occur close to $x-$axis boundary, the effect which is more pronounced during blowing process. The effect of other parameters are presented and well discussed.

KEYWORDS: Arrhenius chemical reaction, Two-dimensional, Dissipative Non-slip, MHD flow, Variable properties.
Mathematics Subject Classification 2020: 76A05, 76D05, 76W05.

I. INTRODUCTION

The study of Two-Dimensional MHD fluid flow has been conducted by several Authors. A fluid flow (motion) at every point parallel to a fixed plane is said to be a two-dimensional flow, this implies that at any given point, the velocity is normal to a fixed plane and this, of course is expected to be constant. Also, the velocity of successive fluid particles at any point is the same at successive period of time. The magnitude and direction of the velocity remains constant at every point. Fluid flow depends on the magnitude of fluid viscosity and the shape of the solid surface of fluid flow and the layer of fluid in the immediate vicinity of a boundary between the solid and the surface of fluid flow where the impact of viscosity is significant is referred to as boundary layer. Aziz etal, [1], studied Steady Boundary Layer Slip Flow along with Heat and Mass Transfer over a Flat Porous Plate Embedded in a Porous Medium, which he concluded that the increase in the permeability and slip parameter causes an increase in heat transfer, but for the case of increase in thermal slip parameter causes a decrease in the heat transfer. Animasaun,[2] examined the 47nm alumina-water nanofluid flow within boundary formed on upper horizontal surface of paraboloid of revolution alongside quartic autocatalysis chemical reaction. He came out with the conclusion that higher value of volume fraction/heat capacity and other properties of 47nm alumina-water nanofluid greatly generate more heat energy which account for overshoot in energy and momentum function.

Several researchers have carried out studies on Magnetohydrodynamics (MHD) and have reported a wide range of MHD applications. Generally, MHD implies any means of fluid flow that involves conductivity of electricity through magnetic field. Occurrence of magnetic induction produces the electromotive force across an electrical conduction as a result of the interactions between magnetic fields, Animasaun, [2]. The convective MHD flow of second-grade fluid was reported by Hayat and Abbas [3] while Olanrewaju et al. [4] studied the unsteady three-dimensional MHD flow and mass transfer in a porous space in the presence of thermal radiation, in this studies, it is discovered that the impact of the Hartman number and the porosity parameter are qualitatively similar and the thermal boundary layer thickness increases as the prandtl number (Pr) decreases. Bilal etal, [5], examined dissipative slip flow along heat and mass transfer over a vertically rotating cone by way of

International Journal of Advances in Engineering and Management (IJAEM)
Volume 4, Issue 4Apr 2022, pp: 357-371www.ijaem.net ISSN: 2395-5252

Nomenclature

X,y	Cartesian coordinates [m]	T_∞	temperature at the free stream
t	time variable [s]	ρ	density of the fluid
u v	Velocity component along x and y direction[m/s]	q'''	heat source/sink
E_a	activation energy	q_r	radiation heat flux
g	acceleration due to gravity [m/s^2]	k_r	reactivity of chemical reaction
U_∞	free stream velocity	δ	boundary layer thickness
B	uniform magnetic field magnetic strength	σ	electrical conductivity
B_0	magnetic strength	**V**	velocity vector
k_1	permeability of porous medium	R	Reynold number
β_c	concentration expansion coefficient	R_A	Arrhenius chemical reaction
β_τ	volume expansion coefficient	H	Hartmann number
C	nanoparticles concentration within the boundary	Gr	Grashof number
C_∞	concentration in the free stream	N	Buoyancy ration
C_p	specific heat at constant pressure	Fs	Forchiemann parameter
E	electric field intensity	ϵ	Positive number $0 < \epsilon \ll 1$
F_m	electromagnetic force	$\bar{\alpha}_{0,1}$	Positive numbers
$f_{x,y}$	body force in x and y direction	R	Reynold number
C_p	specific heat capacity of the fluid	R_G	universal gas constant
$\bar{\lambda}$	Pre-exponential reaction parameter	Sc	Schimidt number
k_T	thermal conductivity	Pr	Prandtl number
T	temperature with the boundary	$\bar{\chi}$	Chemical reaction parameter

chemical reaction with Dufour and soret effects. The study reveals that temperature profile reduces for prandtl number and soret number while increases dufour number and Eckert number. Viscous dissipation is a recent study that has attracted the interest of several researchers across the globe with several applications in the field of science and technology. Dissipation involves transforming heat energy by fluid as a result of the impact of shear forces on the adjacent layers. Its importance cuts across the mechanism of the production of polymer, Aerodynamic heating in the thin boundary layer around high speed aircraft raises the energy of the skin.

On the other hand, non-slip condition is referred to as situation in which viscous fluid flow has no relative velocity with solid surface. This simply means that the relative velocity between the fluid and solid boundary is zero [6]. The non-slip condition occurs when there is high velocity of fluid flow along a curved surface. This brings about boundary layer from solid surface, this process is termed flow separation. Alkahtan etal, [7] investigated the effects of the velocity slip on a viscous dissipation of MHD flow and heat transfer over a thin liquid film on an unsteady stretching sheet. It is discovered from this study that magnetic field suppresses the velocity field which causes enhancement of the temperature profile. Also the viscous dissipation effects is characterized by Eckert number Ec and for wide range of Prandtl number Pr, the effect of viscous dissipation was found to increase the dimensionless free surface temperature for the fluid cooling case, while the impact of viscous dissipation on temperature diminishes in two limit cases $Pr \to 0$ and$Pr \to \infty$

The rate of chemical reaction in a system can be determined by the Arrhenius equation. Arrhenius equation determines the effect of a change of temperature on the rate constant and consequencely on the rate of reaction. Abdulmaleque, [8], studied the influence of binary chemical reaction with activation energy on MHD boundary layer with viscous dissipation and heat generation/absorption. It is observed that increase in activation energy (E)leads to increasing the concentration, temperature and velocity profile. Meanwhile, the rise in the chemical rate constant leads to reduction in the concentration profile and that increasing temperature frequently causes a marked rate of reaction increase. Agaie etal, [9] carried out a research on heat and mass transfer of MHD for an unsteady viscous oscillatory flow. Satya and Dubey, [10] investigated the unsteady MHD heat and mass transfer free convection flow of polar fluid past a vertical moving porous plate in a porous medium with heat generation and thermal diffusion. The study shows that in the absence of magnetic field, the velocity and temperature decreases in water compared with air. Raju etal, [11], investigated the effects of non-uniform heat source/sink and chemical reaction on unsteady

International Journal of Advances in Engineering and Management (IJAEM)
Volume 4, Issue 4Apr 2022, pp: 357-371www.ijaem.net ISSN: 2395-5252

MHD nanofluid flow over a permeable stretching surface. He concluded that raising unsteadiness and reaction parameter depreciates the friction factor. Batti et al. [12] analyzed the heat transfer flow of nanofluid in a channel. They studied the effect of thermal radiation and the MHD effect by using Roseland's approximation, Ohm's law, and Maxwell equations.

Recently, the fluid limiting surface of heat and mass transfer in unsteady natural convection MHD boundary layer flow past a moving plate with binary chemical reaction assumed to move impulsively, with a constant velocity, either in the direction of the flow or in the opposite direction, in the presence of a transverse magnetic field. Both frequency-dependent effects and "long-time" effects that would require non-practically long channels to be observed in steady flow [13]. We also explored mathematically the important aspects of reactive fluid flow, especially the residence time flow behaviour, scale-up and scale-down procedures heat and mass transfer of unsteady MHD natural convective flow past a motioning plate with binary chemical reaction was observed that temperature is enhanced as the fluid angular velocity rises which leads to maximum temperature in the body of the liquid. It is discovered that mean velocity decrease with a rise in the species reaction and reaction order[14]. The computational results for momentum and heat distribution of the flow of nonlinear magnetohydrodynamic (MHD), laminar, viscous, incompressible boundary layer fluid with thermal radiative heat transfer and variable properties past a stretching surface was observed that the parameters which enhanced the heat source terms decreased the fluid viscosity and caused increase in the flow rate [15].An unsteady flow of heat and species transport through a porous medium in an infinite movable vertical permeable flat surface with hydromagnetic chemical reactive fluid flow is stimulated by the thermal and solutant convection, and propelled by the movement of the surface revealed that the species boundary layer increases with a generative chemical reaction and decreases with a destructive chemical reaction [16]. The analysis on the transient double diffusion of a binary mixture in a porous moving flat device without viscoelasticity of the reactive fluid and material deformation, the considered fluid satisfied Newtonian properties with continuous molecular collision under convection and magnetic field influence, the reaction is motivated by chemical heat generation and Arrhenius kinetics, reveal that a monotonically increase in the thermal diffusion is strongly impacted by an increasing value of heat generation and radiation throughout the flow regime.[17]

In this study, our major interest would be to investigate Two-Dimensional Dissipative Non-Slip MHD Flow of Arrhenius Chemical Reaction with Variable Properties. The governing equation would be non-dimensionalised and transformed, hence, analysis would done to show the effect of axial boundary (x), activation energy (ϵ), suction parameter (v_0), drag coefficient (H), Grashof number (Gr), heat generation or absorption parameter (β), chemical reactivity (χ), binary chemical reaction (λ), pressure gradient (G), fluid diffusivity (Sc), buoyancy ratio (N) and fluid conductivity (Pr) on the fluid velocity, temperature and concentration.

II. BOUNDARY LAYER GOVERNING EQUATIONS.

In developing a mathematical theory of boundary layers, the first step is to show the existence, as the Reynolds number R tends to infinity, or the kinematic viscosity ν tends to zero, of a limiting form of the equations of motion, different from that obtained by putting $\nu = 0$ in the first place. A solution of these limiting equations may then reasonably be expected to describe approximately the flow in a laminar boundary layer for which R is large but not infinite. This is the basis of the classical theory of laminar boundary layers.
The full equation of motion for a two-dimensional flow are:

Continuity equation

$$\frac{\partial u}{\partial x} + \frac{\partial v}{\partial y} = 0 \tag{1}$$

x-momentum equation

$$\frac{\partial u}{\partial t} + u\frac{\partial u}{\partial x} + v\frac{\partial u}{\partial y} = -\frac{1}{\rho}\frac{\partial p}{\partial x} + \nu\left[\frac{\partial^2 u}{\partial x^2} + \frac{\partial^2 u}{\partial y^2}\right] + \frac{1}{\rho}f_x(u, T, C, t) \tag{2}$$

y-momentum equation

International Journal of Advances in Engineering and Management (IJAEM)
Volume 4, Issue 4Apr 2022, pp: 357-371www.ijaem.net ISSN: 2395-5252

$$\frac{\partial v}{\partial t}+u\frac{\partial v}{\partial x}+v\frac{\partial v}{\partial y}=-\frac{1}{\rho}\frac{\partial p}{\partial y}+\nu\left[\frac{\partial^2 v}{\partial x^2}+\frac{\partial^2 v}{\partial y^2}\right]+\frac{1}{\rho}f_y(u,T,C,t) \tag{3}$$

Energy transfer equation

$$\rho c_p\left(\frac{\partial T}{\partial t}+u\frac{\partial T}{\partial x}+v\frac{\partial T}{\partial y}\right)=\frac{\partial}{\partial y}\left(k_T\frac{\partial u}{\partial y}\right)+\mu\left(\frac{\partial u}{\partial y}\right)^2-q''' \tag{4}$$

Mass transfer (species) equation

$$\rho\left(\frac{\partial C}{\partial t}+u\frac{\partial C}{\partial x}+v\frac{\partial C}{\partial y}\right)=D\frac{\partial^2 C}{\partial y^2}+\gamma(C-C_\infty)-R_A \tag{5}$$

Where $f_{x,y}(u,T,C,t)$ is the body force in $x-$ and $y-$directions respectively, q''' is non-uniform heat source/sink and are defined by

$$f_x(u,T,C,t)=+g\left(\beta_\tau(T-T_\infty)+\beta_c(C-C_\infty)\right)-\frac{\sigma\mu B^2(x)}{k}(u-U)\mp g\left(\frac{K_1}{\nu}\right)|\hat{u}|(u-U) \tag{8}$$

$$f_y(u,T,C,t)=-\frac{\sigma\mu B^2(x)}{k}v \tag{9}$$

$$q'''=\left(\frac{\kappa u_w(x)}{x\nu}\right)\left[\frac{A^*(T_w-T_\infty)}{bx}(u-U)+B^*(T-T_\infty)\right] \tag{10}$$

$$V_T=\frac{k'\nu}{\tau}\frac{\partial T}{\partial y} \tag{11}$$

$$R_A=k_r^2(T-T\infty)^r\exp\left(-\frac{E_a}{R_G T}\right)(C-C_\infty) \tag{12}$$

$$K_T=k\frac{T}{T_\infty} \tag{13}$$

The thermal boundary conditions depend on the type of heating process under consideration. In the present investigation, the heat transfer analysis has been carried out heating processes namely Prescribed Surface Temperature (PST).

We now define conveniently the following dimensionless quantities;

$$\left.\begin{aligned}x'=\frac{x}{L},y'=\frac{y}{\delta},u'=\frac{u}{U},v'=\frac{v}{U}\frac{L}{\delta},t'=\frac{tv_0^2}{4\nu}\left(\text{or } t\frac{U}{L}\right),U'=\frac{U}{U_0},\omega'=\frac{4\omega\nu}{v_0^2},p'=\frac{p}{\rho U^2},\\(T-T_\infty)=\left(\frac{E_a}{R_G T_\infty^2}\right)^{-1}\theta(t,x,y),(C-C_\infty)=(C_w-C_\infty)\phi(t,x,y),V=\frac{U_1}{U_0}\end{aligned}\right\} \tag{14}$$

where L is the horizontal length scale, δ is the boundary layer thickness at $x=L$, which is unknown. We will obtain an estimate for it in terms of the Reynolds number R. U is the flow velocity, which is aligned in the $x-$direction parallel to the solid boundary.

Now using equation (8) – (13) in equations (2) – (5), momentum in x- and y- directions, energy and species equations becomes

$$\left.\begin{aligned}\frac{\partial u}{\partial t}+u\frac{\partial u}{\partial x}+v\frac{\partial u}{\partial y}=-\frac{1}{\rho}\frac{\partial p}{\partial x}+\nu\left[\frac{\partial^2 u}{\partial x^2}+\frac{\partial^2 u}{\partial y^2}\right]=-\frac{\sigma\mu B^2(x)}{\rho}(u-U)\mp g\left(\frac{K_1}{\nu}\right)|\hat{u}|(u-U)\\+g\left(\beta_\tau(T-T_\infty)+\beta_c(C-C_\infty)\right)\end{aligned}\right\} \tag{15}$$

$$\left.\frac{\partial v}{\partial t}+u\frac{\partial v}{\partial x}+v\frac{\partial v}{\partial y}=-\frac{1}{\rho}\frac{\partial p}{\partial y}+\nu\left[\frac{\partial^2 v}{\partial x^2}+\frac{\partial^2 v}{\partial y^2}\right]-\frac{\sigma\mu B^2(x)}{\rho}v\right\} \tag{16}$$

International Journal of Advances in Engineering and Management (IJAEM)
Volume 4, Issue 4Apr 2022, pp: 357-371www.ijaem.net ISSN: 2395-5252

$$\left.\begin{aligned}\rho c_p\left(\frac{\partial T}{\partial t}+u\frac{\partial T}{\partial x}+v\frac{\partial T}{\partial y}\right)=\frac{\partial}{\partial y}\left(k\frac{T}{T_\infty}\frac{\partial u}{\partial y}\right)-\left(\frac{\kappa u_w(x)}{x\nu}\right)\left[\frac{A^*(T_w-T_\infty)}{bx}(u-U)\right.\\ \left.+B^*(T-T_\infty)\right]+\mu\left(\frac{\partial u}{\partial y}\right)^2\end{aligned}\right\} \quad (17)$$

$$\rho\left(\frac{\partial C}{\partial t}+u\frac{\partial C}{\partial x}+v\frac{\partial C}{\partial y}\right)=D\frac{\partial^2 C}{\partial y^2}+\gamma(C-C_\infty)-k_r^2(T-T\infty)^r\exp\left(-\frac{E_a}{R_G T}\right)(C-C_\infty) \quad (18)$$

Now, using the dimensionless quantities (14), we have the non-dimensional form of the governing equations after dropping primes are

$$\frac{\partial u}{\partial x}+\frac{\partial v}{\partial y}=0 \quad (19)$$

$$\frac{\partial u}{\partial t}+u\frac{\partial u}{\partial x}+v\frac{\partial u}{\partial y}=-\frac{\partial p}{\partial x}+\frac{1}{R}\frac{\partial^2 u}{\partial x^2}+\frac{\partial^2 u}{\partial y^2}-Ha(u-1)\mp Fs(u-1)+Gr\big(N\theta(x,y)+\emptyset(x,y)\big) \quad (19)$$

$$\frac{1}{R}\left(\frac{\partial v}{\partial t}+u\frac{\partial v}{\partial x}+v\frac{\partial v}{\partial y}\right)=-\frac{\partial p}{\partial y}+\frac{1}{R}\frac{\partial^2 u}{\partial x^2}+\frac{1}{R^2}\frac{\partial^2 u}{\partial y}=-\frac{1}{R}Ha \quad (20)$$

$$\frac{\partial\theta}{\partial t}+u\frac{\partial\theta}{\partial x}+v\frac{\partial\theta}{\partial y}=\frac{1}{Pr}\frac{\partial}{\partial y}\left((1+\epsilon\theta)\frac{\partial\theta}{\partial y}\right)+\beta\left(\frac{\partial u}{\partial y}\right)^2-\alpha_o[\alpha_1(u-1)+\theta] \quad (21)$$

$$\frac{\partial\phi}{\partial t}+u\frac{\partial\phi}{\partial x}+v\frac{\partial\phi}{\partial y'}=\frac{1}{Sc}\frac{\partial^2\phi}{\partial y^2}+\chi\phi-\epsilon\lambda\theta^r\exp\left(\frac{\theta}{1+\epsilon\theta}\right)\phi \quad (22)$$

Reynolds number (R) is defined here as

$$R=\frac{UL}{\upsilon},\frac{R_G T_\infty}{E_a}=\epsilon \quad (23)$$

In the limit $R\to\infty$, the equations above reduced to:

$$\frac{\partial u}{\partial x}+\frac{\partial v}{\partial y}=0 \quad (24)$$

$$\frac{\partial u}{\partial t}+u\frac{\partial u}{\partial x}+v\frac{\partial u}{\partial y}=-\frac{\partial p}{\partial x}+\frac{1}{R}\frac{\partial^2 u}{\partial x^2}+\frac{\partial^2 u}{\partial y^2}-Ha(u-1)\mp Fs(u-1)+Gr\big(N\theta(x,y)+\emptyset(x,y)\big) \quad (25)$$

$$\frac{\partial u}{\partial t}+u\frac{\partial u}{\partial x}+v\frac{\partial u}{\partial y}=-\frac{\partial p}{\partial x}+\frac{\partial^2 u}{\partial y^2}-H(u-1)\mp Fs(u-1)+Gr(N\theta(y)+\emptyset(y)) \quad (26)$$

$$0=-\frac{\partial p}{\partial y} \quad (27)$$

$$\frac{\partial\theta}{\partial t}+u\frac{\partial\theta}{\partial x}+v\frac{\partial\theta}{\partial y}=\frac{1}{Pr}\frac{\partial}{\partial y}\left((1+\epsilon\theta)\frac{\partial\theta}{\partial y}\right)+\beta\left(\frac{\partial u}{\partial y}\right)^2-\alpha_o[\alpha_1(u-1)+\theta] \quad (28)$$

$$\frac{\partial\phi}{\partial t}+u\frac{\partial\phi}{\partial x}+v\frac{\partial\phi}{\partial y'}=\frac{1}{Sc}\frac{\partial^2\phi}{\partial y^2}+\chi\phi-\epsilon\lambda\theta^r\exp\left(\frac{\theta}{1+\epsilon\theta}\right)\phi \quad (29)$$

The thermo-fluid physical terms are respectively described as follows:

$$\left.\begin{aligned}\frac{\sigma\mu B^2(x)L}{kU}=H,\frac{g\beta_c(C_w-C_\infty)L}{U^2}=Gr,\frac{\beta_\tau R_G T_\infty^2 L}{\beta_c E_a(C_w-C_\infty)U^2}=N,D\frac{L}{\rho U}=\frac{1}{Sc}\\ R=\frac{UL}{\upsilon},\frac{R_G T_\infty}{E_a}=\epsilon,\mu\frac{UL}{\delta^2}\frac{E_a}{R_G T_\infty^2}=\bar{\beta},\frac{LB^*}{U}\left(\frac{\kappa u_w(x)}{x\nu}\right)=\bar{\alpha}_0,\frac{A^*(T_w-T_\infty)E_a U}{B^* bx R_G T_\infty^2}=\alpha_1\\ \frac{k}{\rho c_p}\frac{L}{U\delta^2 T_\infty}=\bar{\tau},\gamma\frac{L}{\rho U}=\bar{\chi},g\left(\frac{K_1}{\nu}\right)\frac{L}{U}|\hat{u}|=Fs,\ k_r^2\frac{L}{\rho U}\left(\frac{R_G T_\infty^2}{E_a}\right)^{r-1}\exp\left(-\frac{E_a}{R_G T_\infty}\right)=\bar{\lambda}\end{aligned}\right\} \quad (30)$$

The plate is non-porous such that there is no flow across it, that is

$$u=U_1,v=v_w,T=T_w,C=C_w\text{ at }y=0 \quad (31)$$

Far away from the plate outside the boundary layer

$$u\to U\ T\to T_\infty,C\to C_\infty\ as\ y\to\infty \quad (32)$$

International Journal of Advances in Engineering and Management (IJAEM)
Volume 4, Issue 4Apr 2022, pp: 357-371www.ijaem.net ISSN: 2395-5252

III. METHOD OF SOLUTION.

For the flow along a flat plate parallel to the stream velocity U, equation (34) suggest that pressure is independent of y, so the flow for steady motion in the boundary layer is

$$\frac{\partial u}{\partial x} + \frac{\partial v}{\partial y} = 0 \tag{33}$$

$$u\frac{\partial u}{\partial x} + v\frac{\partial u}{\partial y} = -\frac{\partial p}{\partial x} + \frac{\partial^2 u}{\partial y^2} - H(u-1) \mp Fs(u-1) + Gr\big(N\theta(y) + \emptyset(y)\big) \tag{33}$$

$$u\frac{\partial \theta}{\partial x} + v\frac{\partial \theta}{\partial y} = \frac{1}{Pr}\frac{\partial}{\partial y}\left((1+\epsilon\theta)\frac{\partial \theta}{\partial y}\right) + \beta\left(\frac{\partial u}{\partial y}\right)^2 - \alpha_o[\alpha_1(u-1)+\theta] \tag{35}$$

$$u\frac{\partial \phi}{\partial x} + v\frac{\partial \phi}{\partial y'} = \frac{1}{Sc}\frac{\partial^2 \phi}{\partial y^2} + \chi\phi - \epsilon\lambda\theta^r \exp\left(\frac{\theta}{1+\epsilon\theta}\right)\phi \tag{36}$$

The corresponding boundary conditions become:

$$\begin{gathered} u' = V, v' = 0, \theta(x,0) = 1, \phi(x,0) = 1, \\ u' \to 1, \theta \to 0, \phi \to 1 \ as \ y \to \infty \end{gathered} \tag{37}$$

Where

$$V = \frac{U_1}{U_0}, \tag{38}$$

Equation (34) imply that pressure term is independent of y. These conditions demand an infinite gradient in speed at the leading edge $x = y = 0$, which implies a singularity in the mathematical solution there. However, the assumptions implicit in the boundary layer approximation break down for the region of slow flow around the leading edge. The solution given by the boundary layer approximation is not valid at the leading edge. It is valid downstream of the point $x = 0$.

We employed mathematical software *Maple* is used to implicitly compute the numerical solution and displayed the plot of the solution. We make use of y, x −based Solver which uses the default method, which is a centered implicit scheme. The PDE systems are written sufficiently close to a standard form for the method to find the numerical solution. The system of equations considered here has to be solved in the infinite domain$0 < y < y_\infty$. A finite domain in the y −direction can be used instead with y chosen large enough to ensure that the solutions are not affected by imposing the asymptotic conditions at a finite distance. Grid-independence studies show that the computational domain $0 < y < y_\infty$ can be divided into intervals each of uniform step size which equals 0.02. This reduces the number of points between $0 < y < y_\infty$ without sacrificing accuracy.

IV. DISCUSSION OF RESULT

The results of implementing the above Maple inbuilt solve these are displayed in graphical as shown below and discussed. Figure 1-3 indicate the effect of suction $(v_0 < 0)$ and blowing $(v_0 > 0)$ on velocity, temperature and species concentration. It is observed from Figure1(a) that during suction, velocity increases along axial coordinate but rises along longitudinal coordinate until ambient velocity is attained. Similar occurrence was noticed during blowing with unsteadiness along longitudinal axis when the distance along axial coordinate between zero and 1unit as depicted in Figure 1(b). In Figure 2(a), flash increase in temperature was observed in energy content of the flow when the axial coordinate is around 0.5 unit after which it decreases steadily along the axis, while the temperature decreases along longitudinal axis. As a result of blowing, we observed in Figure 2(b) uneven increase intemperature along the axial coordinate around 2 units from the wall beyound which temperature decline steadily. Figure 3(a) depict the effect of suction on species concentration, it could be observec that suction initially enhanced the species contration close to the surface along axial coordinate but consumed away from the wall thereby decreases the concentration staedily both in axial and longitudinal coordinates. While in Figure 3(b), we observed that species concentration decreases sharply far away from the wall along longitudinal coordinate when the flow is just about 2 units along axial coordinate. The flow variables distributions relative to the distance from axial boundary is depicted in the Figures below. The analysis is carried out for suction. Figure 4(a) depict the velocity distribution at various points along the axial boundary. It was observed from the Figure 4(a) that as axial boundary parameter x increases, velocity increases both at the wall and the free stream. Also, Figure 4(b) shows the species distribution at various

International Journal of Advances in Engineering and Management (IJAEM)
Volume 4, Issue 4Apr 2022, pp: 357-371www.ijaem.net ISSN: 2395-5252

point along axial boundary, it is observed that the species distribution exhibit a sinusoidal wave pattern due to increase in the axial boundary parameter x. which means the species distribution has a characteristics of fluctuation as a result of increase in the axial boundary parameter x. Figure 5(a) and (10) shows the energy distribution at various points along axial boundary and variation of activation energies with concentration distribution respectively. It was observed in Figure 5(a) that the profile exhibits a sinusoidal pattern, which means that the floe energy fluctuates at every point when as axial boundary parameter increases. On the other, in Figure 5(b), it could be seen that there is a decline in concentration as the activation energy parameter increases, which correlate with Muhammad and Zaheer [18].

Figure 6(a) and (b) shows the effect of suction parameter on the velocity and concentration distribution. From Figure 6(a), it is observed that the increase in the suction parameter results in the increase in velocity at the wall, decreases away from the wall and shows no significant effect at the free stream. This means that velocity varies at every point when the suction parameter is increased. Also, Figure 6(b) shows a significant effect at all point, i.e. when the suction parameter increases, the concentration increases at every point. Figure 7(a) and (b) shows the effect of Drag Coefficient H and the buoyancy parameter Gr on velocity distribution respectively. From Figure 7(a), the velocity shows a slight increase in velocity at the wall and decreases in velocity at the free stream with increase in the drag coefficient H, which indicates that the velocity of the fluid varies at every point of the flow.

Also, from Figure 7(b), the velocity increases at the wall and away from the wall, while the velocity decreases at the free stream with the increase in the Grashof number Gr which correlates with Okedoye and Salawu [14].Figure 8(a) and (b) shows the effect of variation of the buoyancy parameter on concentration and temperature distribution. It is observed from Figure 8(a) that the increase in the buoyancy factor parameter (Gr) leads to the decrease in the concentration of the fluid at every point. Figure 8(b), shows an increase in temperature at the wall, decrease in temperature at the wall, away from wall and show no significant effect at the free stream. Figure 9(a) and (b) is the effect of the variation of Homic heating and variation of heat generation or absorption on temperature distribution respectively. From Figure 9(a), it is observed that the increase in the Homic heating parameter α_0 causes the decrease in temperature at every point. From Figure 9(b), there is an increase in the temperature at every point due to the increase in the heat generation/absorption parameter β.

Figure 10(a) and (b) shows the effect of chemical reactivity parameter on the velocity and concentration distribution. It is shown from Figure (a) that the increase in the chemical reactivity parameter χ brings about the increase in velocity profile from the wall and shows no significant effect at the free stream. Also, Figure (b) shows the increase in the concentration at every point. Figure 11(a) and (b) shows the effect of binary chemical reaction parameter λ on velocity and concentration distribution respectively. From Figure 11(a), the momentum boundary layer at every point decline as the binary chemical reaction increases, so also the binary chemical reaction was observed to diminish the concentration boundary layer at all point. Figure 12(a) and (b) shows the effect of buoyancy ratio on the velocity and concentration distribution respectively. It is observed from Figure 12(a) that velocity decreases as the buoyancy ratio increases, while the concentration increases boundary layer was observed to increase as the buoyancy ratio increased. Figure 13(a) and (b), depict the effect of the variation of pressure gradient G on velocity and concentration respectively.

From Figure 13(a), it is observed that the increase in the pressure gradient leads to the increase in the velocity. It could also be deduced from the figure that, at each value of pressure gradient, a maximum velocity was attained which was also maintained for some distance before declining to ambient velocity of the flow, and from Figure 13(b), the concentration boundary layer diminishes as the pressure gradient is increases.

International Journal of Advances in Engineering and Management (IJAEM)
Volume 4, Issue 4Apr 2022, pp: 357-371www.ijaem.net ISSN: 2395-5252

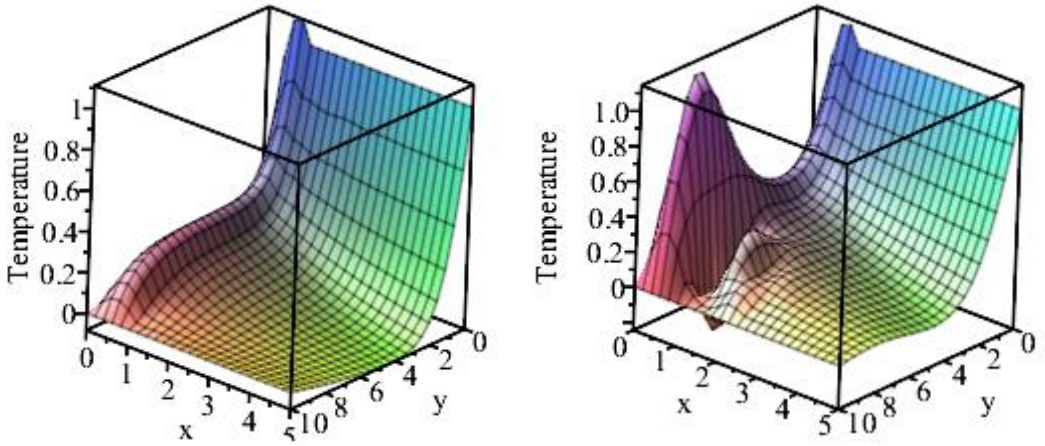

a *b*

Figure 1: 2D Velocity Distribution for (a) suction; (b) blowing

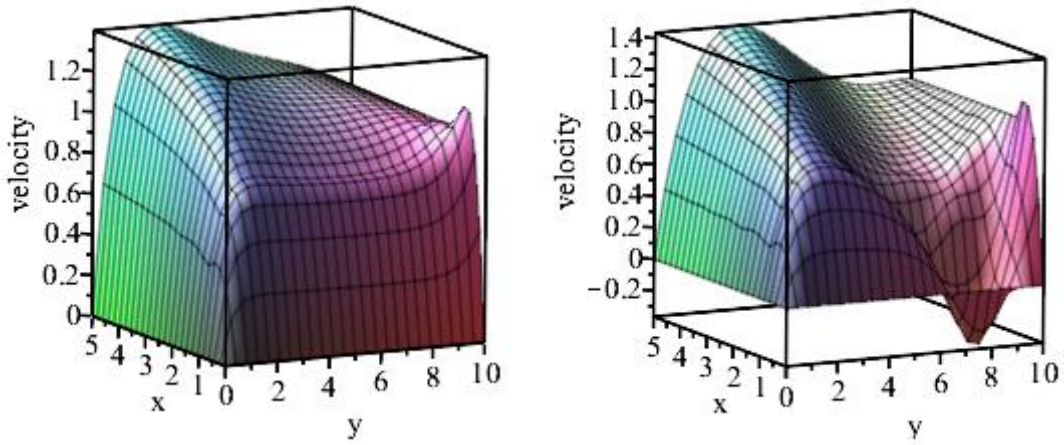

a *b*

Figure 2: 2D Energy Distribution for (a) suction; (b) blowing

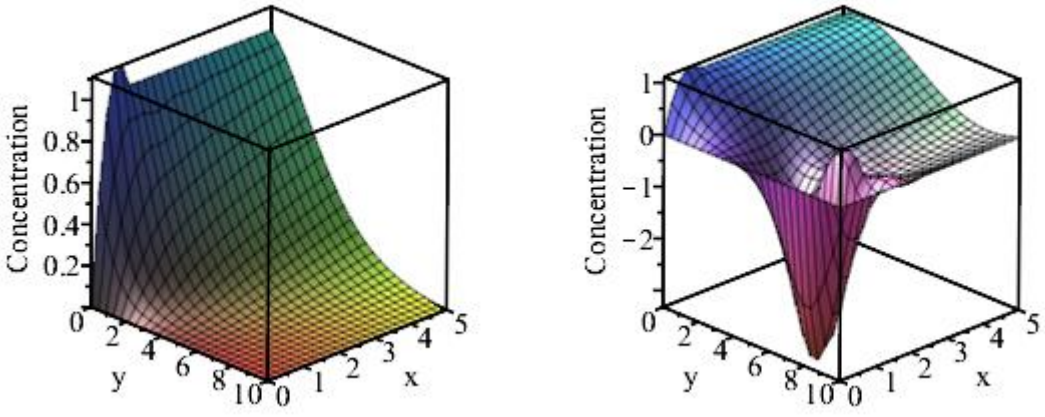

a *b*

Figure 3: 2D Species Distribution for (a) suction; (b) blowing

International Journal of Advances in Engineering and Management (IJAEM)
Volume 4, Issue 4Apr 2022, pp: 357-371www.ijaem.net ISSN: 2395-5252

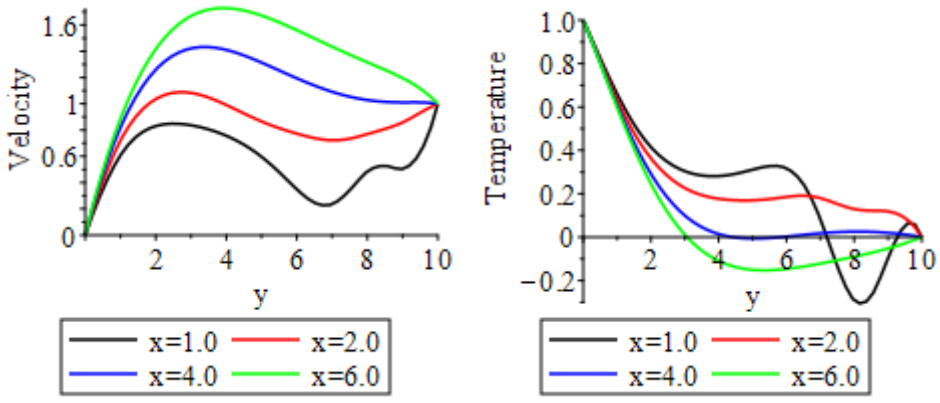

a *b*

Figure 4: (a) Energy distribution at various points along axial boundary; (b) Variation of activation energies with Concentration distribution

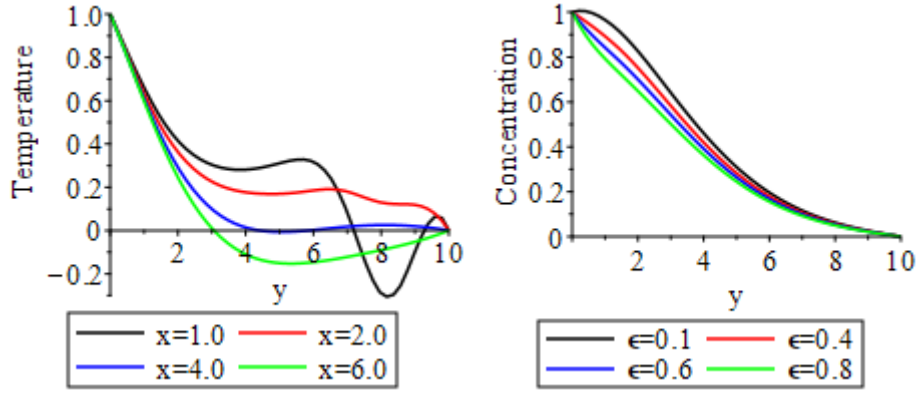

a *b*

Figure 5: (a) Energy distribution at various points along axial boundary; (b) Variation of activation energies with Concentration distribution

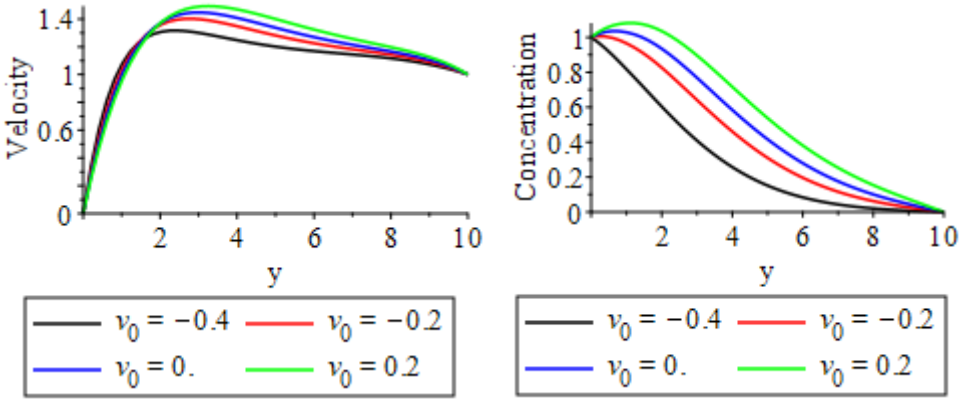

a *b*

Figure 6: Variation of suction parameter (a) velocity distribution; (b) species distribution

International Journal of Advances in Engineering and Management (IJAEM)
Volume 4, Issue 4Apr 2022, pp: 357-371www.ijaem.net ISSN: 2395-5252

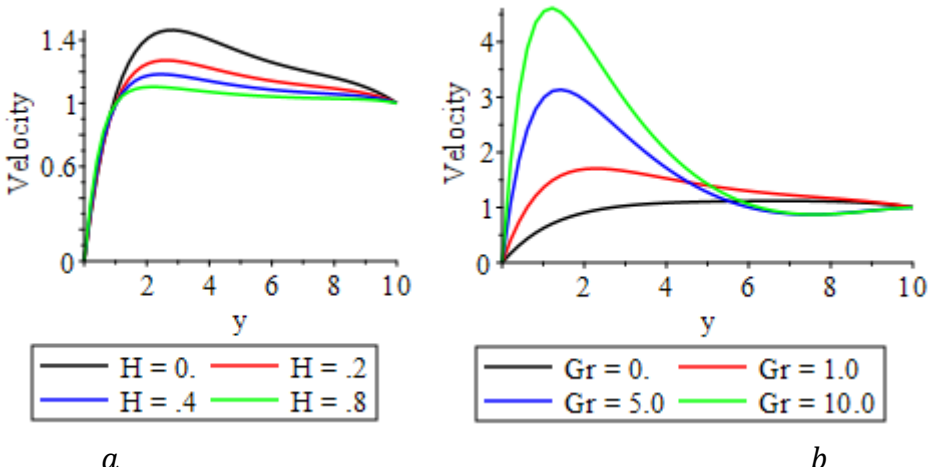

a *b*

Figure 7: Variation of velocity with (a) of drag coefficient on; (b) buoyancy factor

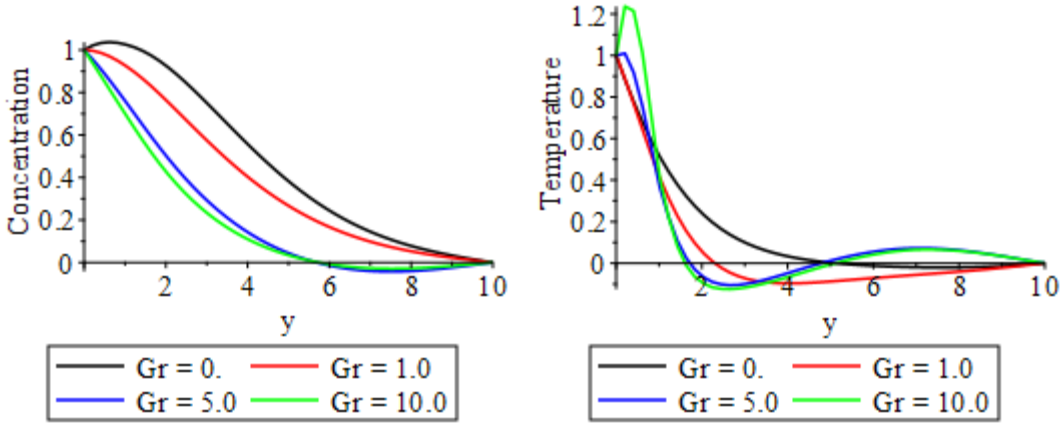

a *b*

Figure 8: Variation of buoyancy factor with (a) species concentration; (b) temperature distribution

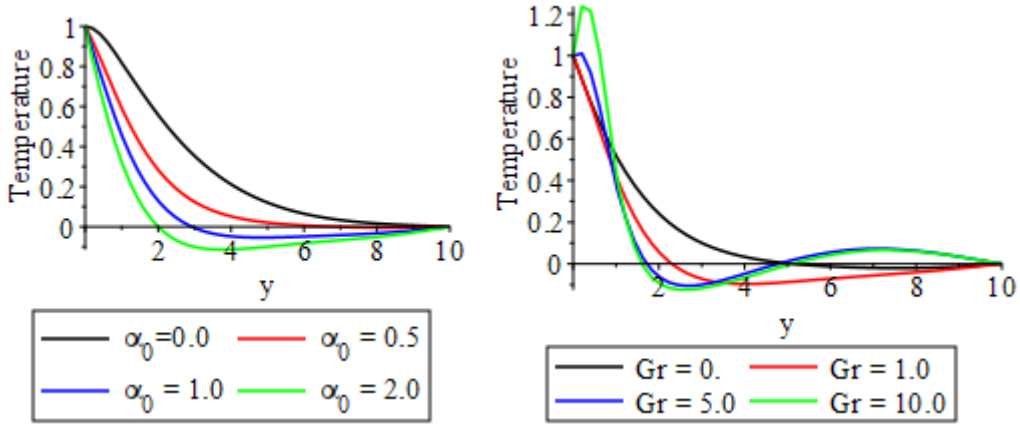

a *b*

Figure 9: Variation of temperature with (a) homic heating; (b) heat generation/absorption

International Journal of Advances in Engineering and Management (IJAEM)
Volume 4, Issue 4Apr 2022, pp: 357-371www.ijaem.net ISSN: 2395-5252

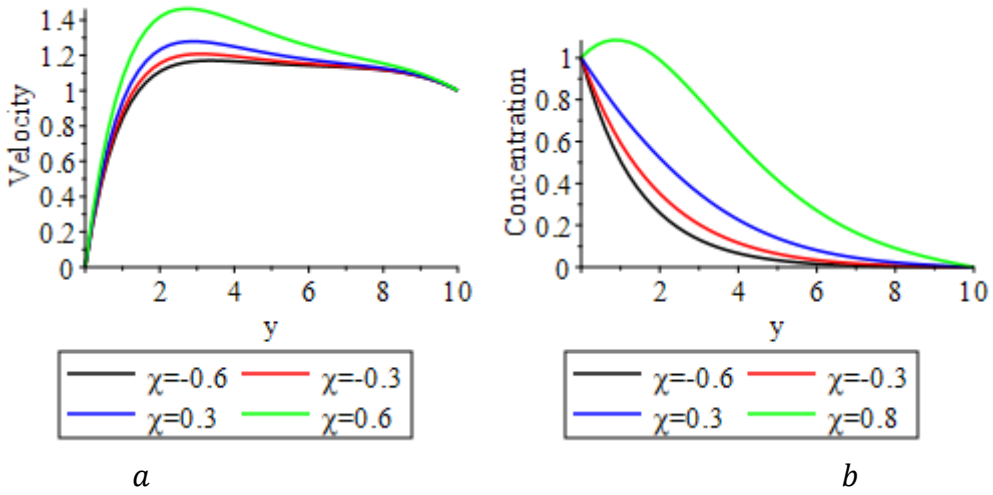

a *b*

Figure 10: Variation of chemical reactivity parameter on (a) velocity distribution; (b) species concentration.

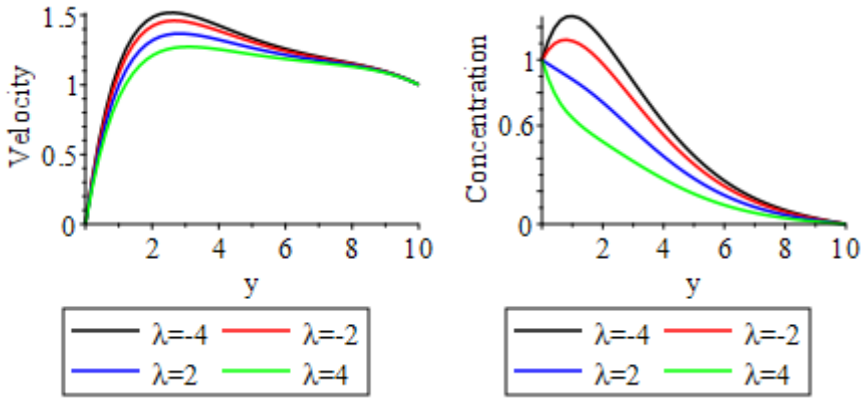

a *b*

Figure 11: Variation of velocity with (a) binary chemical parameter; (b) species distribution

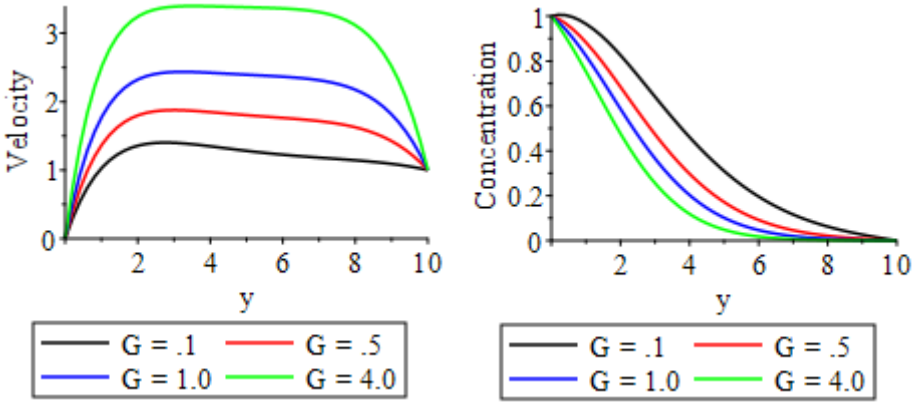

a *b*

Figure 12: Variation of buoyancy ratio on (a) velocity distribution; (b) species distribution

International Journal of Advances in Engineering and Management (IJAEM)
Volume 4, Issue 4Apr 2022, pp: 357-371www.ijaem.net ISSN: 2395-5252

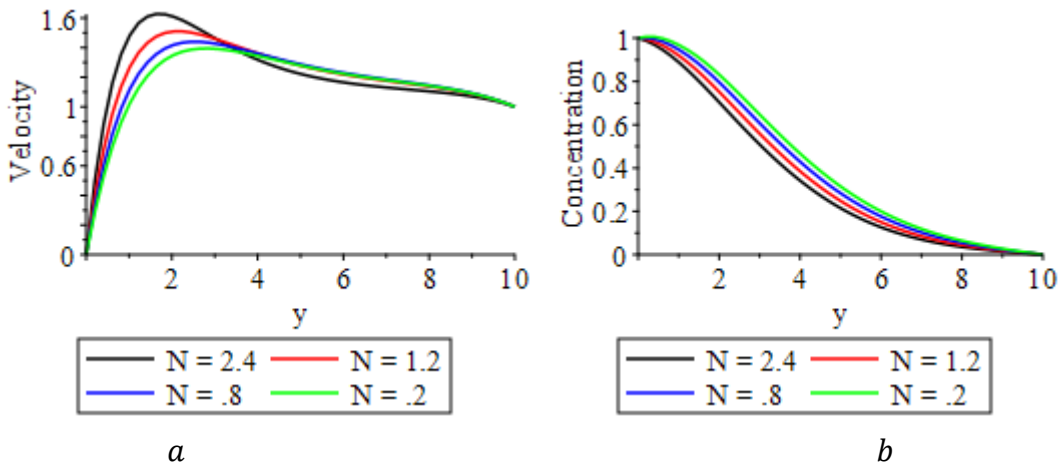

a *b*

Figure 13: Variation of pressure gradient on (a) velocity distribution; (b) species distribution

V. CONCLUSION

Two-Dimensional Dissipative Non-Slip MHD Flow of Arrhenius Chemical Reaction with Variable observations. Hence, the following conclusions has been reached in the study;

- An increase in the axial boundary parameter (x) leads to the increase in the velocity at the wall and at the free stream, while the energy and chsmical species distribution exhibit a characteristics of fluctuation due to the increase in the axial boundary parameter (x).
- There is a decrease in concentration as the activation energy parameter increases.
- The increase in the suction parameter (v_0) results in the increase in velocity at the wall, decreases away from the wall and shows no significant effect at the free stream. This means that velocity varies at every point when the suction parameter is increased. Meanwhile, the increase in the suction parameter (v_0), results in the increase of the concentration at every point.
- The velocity shows a slight increase in velocity at the wall and decrease in velocity at the free stream with increase in the drag coefficient (H), which indicates that the velocity of the fluid varies at every point of the flow.
- The velocity increases at the wall and away from the wall, while the velocity decreases at the free stream with the increase in the Grashof number (Gr).
- The increase in the buoyancy factor parameter (Gr) leads to the decrease in the concentration of the fluid at every point. Increase in temperature at the wall and decrease in temperature away from the wall.
- The increase in the chemical reactivity parameter (χ) brings about the increase in velocity profile from the wall and shows no significant effect at the free stream and increase in the concentration profile at every point.
- The increase in the Homic heating parameter (α_0) causes the decrease in temperature at every point.
- There is an increase in the temperature at every point due to the increase in the heat generation/absorption parameter(β).
- The velocity and concentration decreases at every point as the binary chemical reaction increases(λ).
- The increase in the pressure gradient (G) leads to the increase in the velocity at every point and the concentration decrease at all point as the pressure gradient is increased.
- The temperature decreases at every point as the fluid conductivity parameter (Pr) increases.

VI. CONCLUSION

Two-Dimensional Dissipative Non-Slip MHD Flow of Arrhenius Chemical Reaction with Variable observations. Hence, the following conclusions has been reached in the study;

- An increase in the axial boundary parameter (x) leads to the increase in the velocity at the wall and at the free stream, while the energy and chsmical species distribution exhibit a characteristics of fluctuation due to the increase in the axial boundary parameter (x).
- There is a decrease in concentration as the activation energy parameter increases.
- The increase in the suction parameter (v_0) results in the increase in velocity at the wall, decreases away from the wall and shows no significant effect at the free stream. This means that velocity varies at every point when the suction parameter is increased. Meanwhile, the

increase in the suction parameter (v_0), results in the increase of the concentration at every point.

- The velocity shows a slight increase in velocity at the wall and decrease in velocity at the free stream with increase in the drag coefficient (H), which indicates that the velocity of the fluid varies at every point of the flow.
- The velocity increases at the wall and away from the wall, while the velocity decreases at the free stream with the increase in the Grashof number (Gr).
- The increase in the buoyancy factor parameter (Gr) leads to the decrease in the concentration of the fluid at every point. Increase in temperature at the wall and decrease in temperature away from the wall.
- The increase in the chemical reactivity parameter (χ) brings about the increase in velocity profile from the wall and shows no significant effect at the free stream and increase in the concentration profile at every point.
- The increase in the Homic heating parameter (α_0) causes the decrease in temperature at every point.
- There is an increase in the temperature at every point due to the increase in the heat generation/absorption parameter(β).
- The velocity and concentration decreases at every point as the binary chemical reaction increases(λ).
- The increase in the pressure gradient (G) leads to the increase in the velocity at every point and the concentration decrease at all point as the pressure gradient is increased.
- The temperature decreases at every point as the fluid conductivity parameter (Pr) increases.
- The concentration decreases at every point as the fluid diffusivity parameter (Pr) increases.

Conflict of Interests: The authors declare that there is no conflict of interestsregarding the publication of this paper.

REFERENCES

[1] Aziz, A. Siddique, J. I. and Aziz, T. (2014). "Steady Boundary Layer Slip Flow along with Heat and Mass Transfer over a Flat Porous Plate Embedded in a Porous Medium". PLoS ONE 9(12):e114544. doi:10.1371/journal.pone.0114544.

[2] Animasaun I.L. (2016). "47nm alumina-water nanofluid flow within boundary layer formed on upper horizontal surface of paraboloid of revolution in the presence of quartic autocatalysis chemical reaction". Alexandria Engineering Journal (2016) 55, 2375-2389; http://dx.doi.org/10.1016/j.aej.2016.04030

[3] Hayat, T. and Abbas, Z., (2018) "Heat transfer analysis on the MHD flow of a second grade fluid in a channel with porous Medium". Chaos Solitons Fractals**2018**, 38, 556–567.

[4] Olanrewaju, P. O., Olanrewaju, M. A. and Ajadi, D. A. (2011). "Unsteady Three – dimensional MHD flow and mass transfer in a porous space in the presence of thermal radiation". International research journal, vol. 2(2) pp.044-051,

[5] Bilal, S., Khalil, Ur Rehman and Hamayun, (2016). "Dissipative slip flow along heat and mass transfer over a vertically rotating cone by way of chemical reaction with Dufour and Soret effects.", AIP Advance 6,125125(2016). https://doi.org/10.1063/1.4973307

[6] Renuka, P., Ganga, B., Kalaivanan, R. and Abdulhakeem, A. K., (2020). "Slip effect on Ohmic Dissipation non-Newtonian fluid flow in the presence of aligned magnetic field.", Journal of Applied and Computational Mechanics; 6(2)(2020) 296 – 306: DOI: 10.22055/JACM.2019.29024.1543

[7] Alkahtan, B., Subha, A. M. and Aly, E. H., (2016). "Effects of the velocity slip on a viscous dissipation of MHD flow and heat transfer over a thin liquid film on an unsteady stretching sheet."; fis.vol.62 no.6 mexico nov/dic 2016

[8] Abdul Maleque, K. H., (2013). "Effects of binary chemical reaction and activation energy on MHD boundary layer heat and mass transfer flow with viscous dissipation and heat generation/absorption.", ISRN Thermodynamics, vol. 2013, article ID284637: http://dx.doi.org/10.1155/2013/284637

[9] Baba Galadima Agaie, Sani Isa, Ali Shu'aibu, Mai'anguwa and Abubakar Saddiq Magaji, (2021), "Heat and mass transfer of MHD for an unsteady viscous oscillatory flow.", Science world Journal, vol. 16(No.2) 2021, ISSN: 1597 – 6343

[10] Satya Sagar Saxena and Dubey, G. K., (2011). "Unsteady MHD heat and mass transfer free convective flow of polar fluids past a vertical moving porous plate in a porous medium with heat generation and thermal diffusion.", Advances in Applies Science Research, 2011,2(4):259-278; www.pelagiaresearchlibrary.com

[11] Raju, C. S. K. and Sandeep, N., (2016). "Effects of non-uniform heat source/sink and chemical reaction on unsteady MHD nanofluid flow over a permeable stretching surface."Advance Science, Engineering and Medicine, 8(3):1-10. DOI:10.1166/asem.2016.1848

[12]]. Bhatti, M. M., Ahmad, Zeeshan and Rahmat, Ellahi., (2017). "Heat transfer with thermal radiation on MHD particle–fluid suspension induced by metachronal wave." Pramana 89(3):48, DOI:10.101007/s2043-017-1444-6.

{13] A. M. Okedoye and P. O. Ogunniyi (2019): MHD Boundary Layer Flow Past a Moving Plate with Mass Transfer and Binary Chemical Reaction. Journal of the Nigerian Mathematical Society, Vol. 38, Issue 1, pp. 89-121.

[14] A. M. Okedoye and S. O. Salawu (2019): Unsteady oscillatory MHD boundary layer flow past a moving plate with mass transfer and binary chemical reaction. SN Applied Sciences (2019) 1:1586 https://doi.org/10.1007/s42452-019-1463-7.

[15] Akindele M. Okedoye and Sulyman O. Salawu (2019): Effect of Nonlinear Radiative Heat and Mass Transfer on MHD Flow over a Stretching Surface with Variable Conductivity and Viscosity. Journal of the Serbian Society for Computational Mechanics / Vol. 13 / No. 2, 2019 / pp 86-103 (10.24874/jsscm.2019.13.02.07).

[16] A.M. Okedoye and S.O. Salawu (2020): transient heat and mass transfer of hydromagnetic effects on the flow past a porous medium with movable vertical permeablesheet. Int. J. of Applied Mechanics and Engineering, 2020, vol.25, No.4, pp.175-190. DOI: 10.2478/ijame-2020-0057.

[17] Akindele M. Okedoye, Sulyman O. Salawu, and Raphael E. Asibor (2021): a convective MHD double diffusive flow of a binary mixture through an isothermal and porous moving plate with activation energy. Computational Thermal Sciences, 13(5):45–60 (2021).

[18] Muhammad, Azam and Zaheer, Abbas (2021). "Recent progress in Arrhenius Activation Energy for Radiation Heat Transfer cross nanofluid over a melting wedge.", https://doi.org/10.1016/j.jpr.2021.11.004.